EU contract number RII3-CT-2003-506395

CARE-Report-2007-033-NED
edms 883118

CARE NED Work Package 2 "Thermal Studies and Quench Protection"

Final report on Heat transfer study

B. Baudouy, J. Polinski

CEA/Saclay, DSM/DAPNIA, France

Content

1. Introduction

One of the key issues in the operation of a superconducting particle accelerator is the temperature margin of the magnets the most exposed to beam losses and the ability of the cryogenic system to cope with the deposited energies. In the case of LHC, the temperature margins of the superconducting magnet coils operated in superfluid helium (He II) is mainly determined by the heat transfer coefficient through the polyimide insulation (electrical insulation) wrapped around the NbTi-based, Rutherford-type cables [1]. Extensive measurements of this coefficient have been carried out at CEA/Saclay in the 1990's on various types of insulation systems and an optimum solution was chosen for the cables of the LHC arc dipole and quadrupole magnets [2]. Furthermore, the geometry of the cooling channels inside the magnet cold masses as well as the diameters of the pipes connecting the various cryogenic elements were dimensioned to ensure a proper extraction of the energy deposited by beam losses.

Wherever NED-like magnets are implemented, they will be subjected to beam losses, and thereby, to energy depositions, which are likely to be higher than those presently foreseen in the LHC. Furthermore, "wind & react" Nb_3Sn coils call for the use of insulation schemes that are very different from the polyimide wraps applied in LHC magnets and which have never been thoroughly investigated from the thermal point of view. Hence, the issues of temperature margin and magnet cooling must be reassessed to determine what the operational limits of this kind of magnets are.

Since the most probable candidate for cooling such magnets is superfluid helium at atmospheric pressure, a pressurized superfluid helium double cryostat has to be build to achieve the NED thermal study program. The thermal study program for the NED CARE work package 2 is articulated on two experimental apparatuses. Te first one, called the "Stack Experiment", aims to study the heat transfer on a model of a coil with the same environment as in a real magnet. That is to say that this experiment tries to reproduce the mechanical constraints, the geometrical environment and the heat loads. It is composed of a stack of pseudo-conductors where heat is dissipated by Joule effect, electrically insulated like real cables and in a compression mould. The second experimental apparatus aims to study the thermal properties of the electrical insulation itself, without being in the "magnet environment". This apparatus is called the "Drum Experiment" and allows creating 1D heat transfer perpendicular to the cross section of the sample study. If the sample is not permeable to He II than the drum experiment allows to determinate the thermal conductivity and the Kapitza resistance of the electrical insulation.

This report presents the results obtained with the two experimental apparatuses on the electrical insulations developed in the CARE NED program, the conventional insulation made of fiberglass tape fully impregnated with epoxy resin and the innovative insulation made of a fiberglass tape impregnated with a porous precursor. The double bath cryostat build during the NED program and the experimental apparatus are also described in details.

2. The Double bath cryostat

2.1.   *General description and requirements*

The NED cryostat has been designed to perform heat transfer experiments primarily in superfluid helium (He II) in the temperature range of 1.6 K to 2.1 K at atmospheric pressure. But its design also allows to perform experiments at different thermodynamic states such as in normal helium (He I) with a temperature around 4.2 K and around atmospheric pressure and also in supercritical state at a pressure higher than 2.5 atm. These experiments demand a fine

temperature regulation of the helium bath (reference bath) where the tested sample will be located. In the superfluid helium state, the temperature of the reference bath must be regulated within 1 mK over the duration of the test, i.e. an hour. In normal helium the temperature stability margin of the reference bath is ten times larger, i.e. around 10 mK over the duration of the test. For these two thermodynamic states the pressure has to be regulated within a few mbar. For the supercritical state only pressure will be regulated within 10 mbar.

Pressurized superfluid helium is produced from normal helium refrigerated by a saturated He II bath located around it. A Pumping system is used to generate saturated He II (for example: 1.8 K – 16 mbar). This cryostat is based on the principle of the "Claudet bath" described in Figure 1. The pressurized He II bath is maintained at constant temperature by heat exchange with the saturated He II bath located around it and a temperature regulation system. The pressurized He II bath is separated from the 4.2 K bath by a "lambda plate". The saturated He II bath is filled with helium from the 4.2 K helium bath through a thermal heat exchanger. The thermal heat exchanger (gas-liquid: 4.2/1.8 K) is located in the pumping line, for sub-cooling liquid He I and placed before a cryogenic expansion valve (Joule-Thomson valve). The cryostat is able to maintain a pressurized He II bath (and also the 4.2 K bath) up to 3 bars.
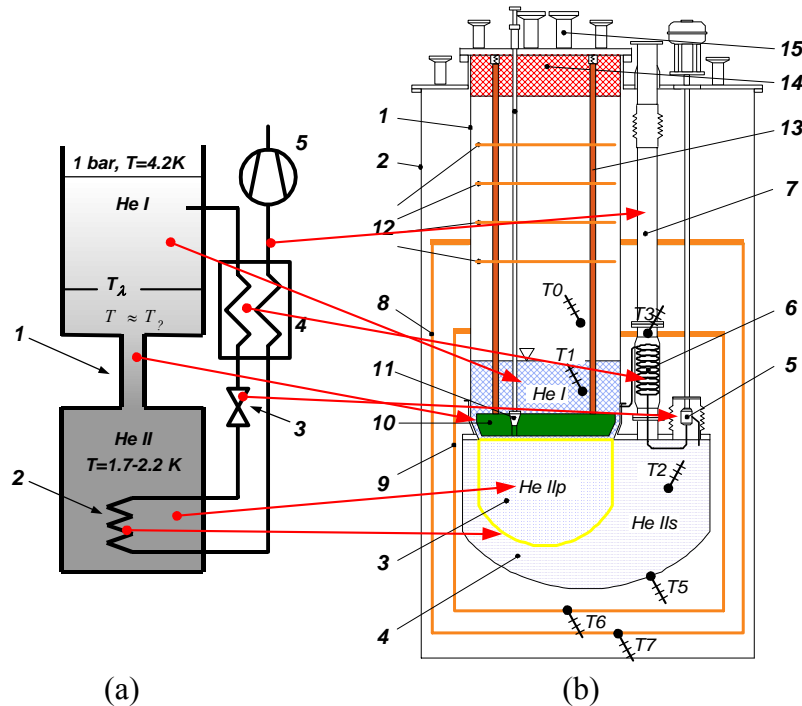

(a)   (b)

Figure 1. a) Claudet bath principle: 1 – constriction, 2 – He IIs/He IIp heat exchanger, 3 – J-T valve, 4 – recuperative heat exchanger, 5 –vacuum pump; b) NED cryostat scheme: 1 – He I vessel, 2 – vacuum container, 3 – He IIp vessel, 4 – He IIs vessel, 5 – J-T valve, 6 – recuperative heat exchanger, 7 – heat exchanger pipe, 8/9 – external/internal radiation shield, 10 – λ-plate, 11 – λ-valve, 12 – insert radiation shields, 13 – λ-plate supports, 14 – foam insulation, 15 – instrumentation ports, T0 – T7 temperature measurement points

CEA Saclay established the specifications of the cryostat in a document edited in 2004 [3]. The design and fabrication of the cryostat was realized and provided by Kriosystem in Poland under supervision of Wroclaw University of Technology [4]. Kriosystem and WUT were responsible for the design and the thermal and mechanical calculations necessary to build the cryostat. The thermal heat exchanger was designed by CEA Saclay and described in

document [5]. Kriosystem manufactured it. Integration of the heat exchanger was under the responsibility of Wroclaw University of Technology. Furthermore, leak tests in liquid helium were also done on the cryostat with the heat exchanger at Wroclaw. Factory test at 4.2 K and provisional acceptance had to be done at Wroclaw University of Technology before shipping. The figure 2 presents the cryostat on its final location at CEA Saclay.

Figure 2. The NED facility at CEA Saclay. The automation and data acquisition system is located on the left. The cryostat itself is located in the middle of the photo and on the right side of the picture one can see the insert with the lambda plate (green piece).

2.2. Thermal stability tests and Performance

The results of stability test are presented in the Figure 3. For the temperature range studied (x-axis), the difference between the temperature set-point and the measurement is within 1 mK (y-axis). The stability of each point is around ±1 mK (error bars) over a duration of over one hour (white frame).

Performance tests have been also realized. The results are presented in the Figure 3 in the orange frame for each temperature. The power presented corresponds to the power dissipated in the heater, located in the pressurized He II vessel, to maintain the temperature of the He II pressurized bath. This power is therefore the power available on the He II vessel to perform a test, i.e. the power that can be dissipated in the test sample. This power was expected to be between 5 W and 10 W and decreasing with temperature.

The stability and the performance obtained with the NED cryostat are acceptable to perform the heat transfer program of NED.
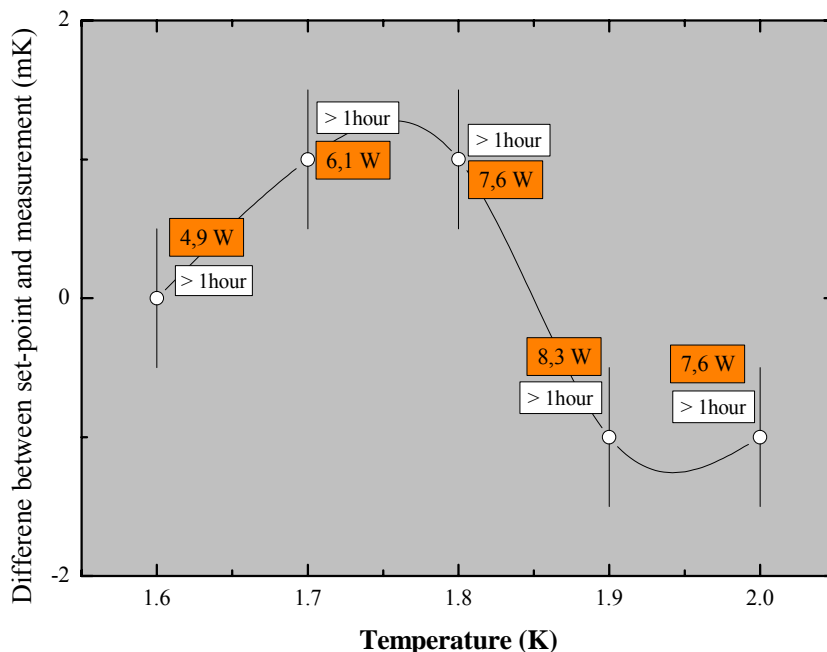
Figure 3. Stability and performance of the NED cryostat

3. Experimental Apparatus

3.1.   *The stack experimental models*

To study heat transfer in superconducting coils of accelerator magnets, it is necessary to reproduce the geometrical, mechanical, electrical and thermal configuration of such a system. Experimental models have been designed to reproduce such a complicated environment and are called "stack" experiments since they reproduce the stack of superconducting cable, insulated and under mechanical constraint as in magnets. Figure 4 shows the two setups used in the NED program to study heat transfer.
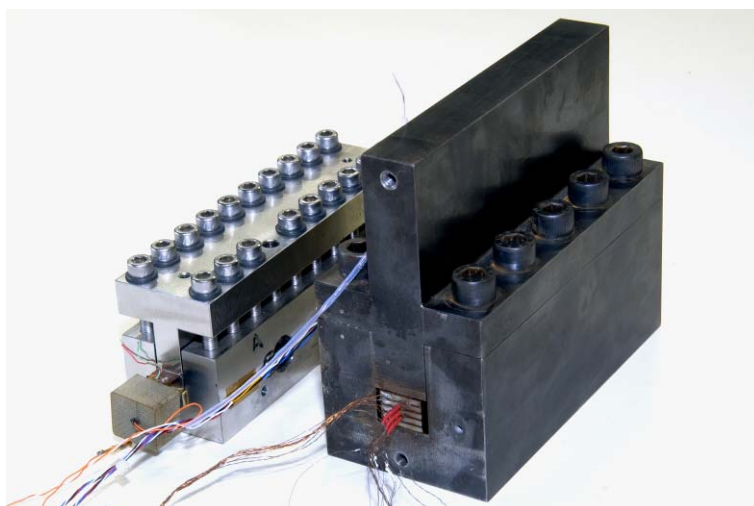

Figure 4. The "stack" experimental models from KEK (left) and Saclay (right).

These two experimental models are very similar, only the dummy conductor, representing the superconducting cable, is different. Both are composed of a mechanical mould that creates

mechanical constraints (only in compression) of a magnet. The stack is composed of five conductors instrumented with heaters and a central one, which is also instrumented with two thermometers. One, three or five conductors can be heated by Joule effect (electrical current). For the Saclay mould, the superconducting cables (the conductors) are simulated by stainless steel plates, 2.5-mm thick × 17-mm wide × 150-mm long, so as to simulate the beam losses by Joule effect in the conductor volume. The surface of the plates is machined to reproduce the geometry of the cable strands (cf. Figure 5). The ends are not machined in order to ensure the tightness of the insulating tapes and thus prevent any helium leak. In addition, the low heat conductivity of stainless steel makes it possible to avoid end effects due to longitudinal conduction. Allen Bradley type temperature sensors are inserted in cavities specially machined in the plates before being embedded in epoxy resin (cf. Figure 5). Two current leads are soldered to the ends of each conductor so as to dissipate up to 150 mW. It must be noted that the temperature sensors measure the surface temperature of the conductor at the middle of the large face [6].
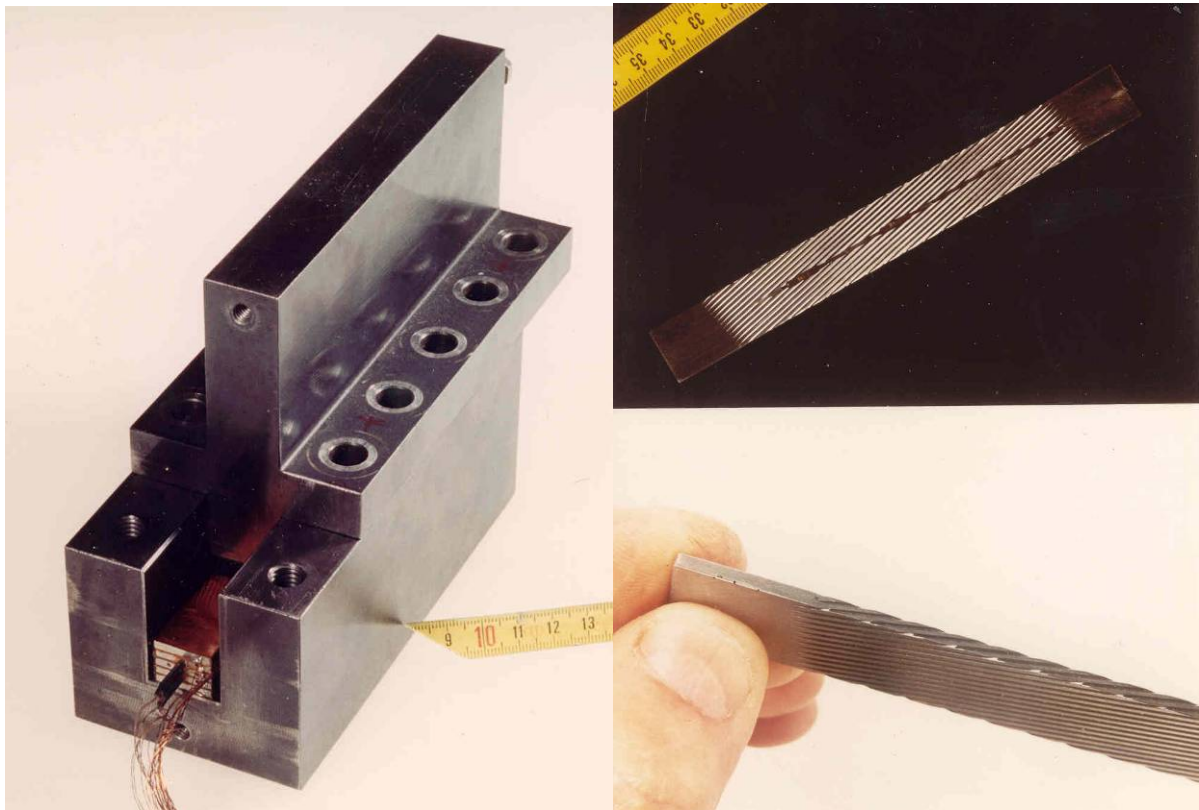

Figure 5. Details of the Saclay "stack experiment".

The sample consists of a stack of five model conductors, insulated and polymerised under temperature and pressure conditions comparable to those of the dipole winding (P = 50 MPa to 150 MPa and θ = 130 °C to 170 °C depending on the material used for secondary wrapping). The sample is then inserted in a clamping system providing a compressive force on the stack ($\approx$ 60 MPa) during the tests in a pressurised He II cryostat.

For the KEK mould the superconducting cables are simulated by cables of CuNi in order to generate Joule heating in the cable. The size of the cable, 1.9 mm thick, 1l mm wide and 150 mm long, with a key-stone angle, is identical to the real superconducting cable for the insertion quadrupole magnet that has been under development at KEK for the LHC. Figure 6

shows the preparation procedures including the location of thermometers and the wrapping of the cable with electrical insulation [7].
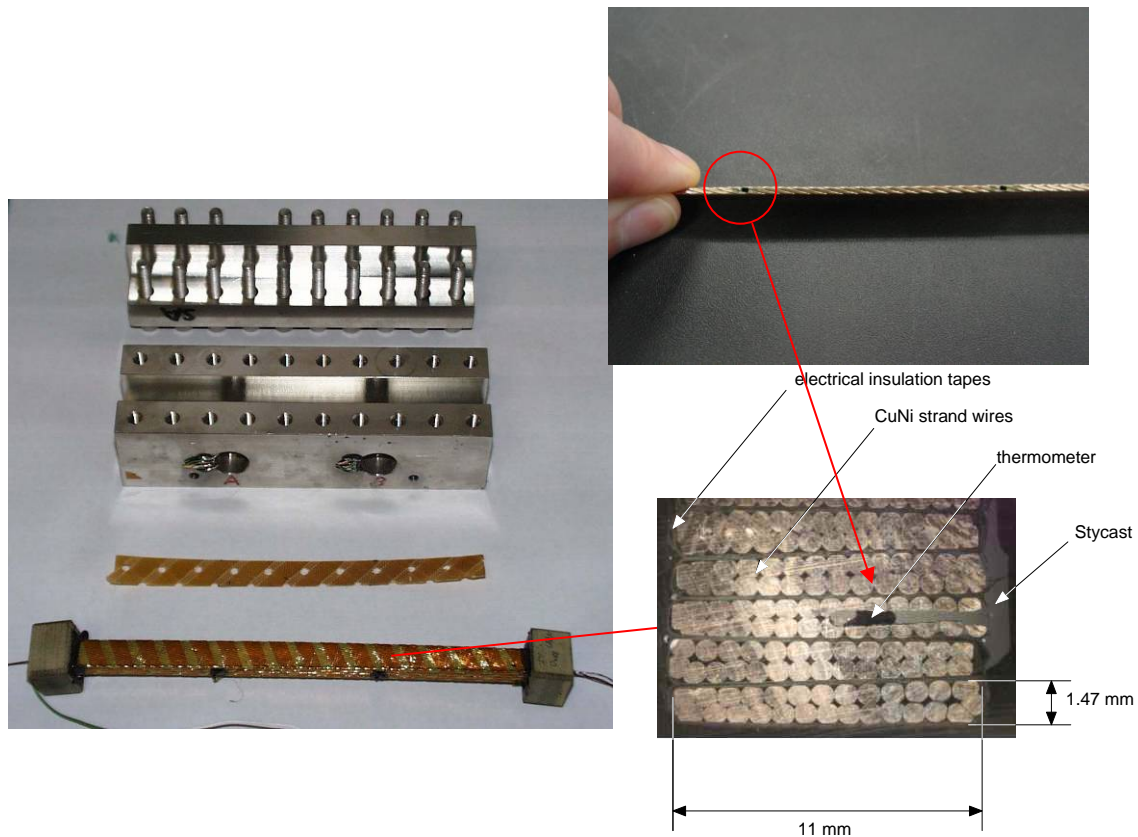

electrical insulation tapes

CuNi strand wires

thermometer

Stycast

1.47 mm

11 mm

Figure 6. Details of the KEK "stack experiment".

The experimental method consists of measuring the increase of the conductor temperature when the heat is dissipated in it. We established heat transfer curve $\Delta T = f(Q)$ as a function of the bath temperature. This measurement allows to establish the overall thermal resistance of the conductor including heat transfer in the conductor, at the interface between the conductor and the helium inside the conductor, through the insulation and the interface between the insulation and the helium in the bath. This experiment serves principally to compare electrical insulation schemes more than predicting the overall heat transfer since no general model exists at this time. Nevertheless, it is an essential tool to test and choose the scheme that is suited for the magnet design.

The in-situ acquisition and calibration system for the temperature sensors, using bare ship cernox thermometers, makes it possible to measure the temperature differences between the conductors and the helium bath with a precision of $\pm$ 1 mK. The conductors are heated individually or collectively by passing a current adjustable from 0 A to 10 A. Their temperature is measured after establishing a stationary regime. The external sample temperature, i.e., the He II bath temperature (1.7 K < T_b < 2. 16 K), is controlled and constant for all the studied power range.

3.2.   The drum experimental model

3.2.1. Experimental method

The goals of the measurements are to determine the thermal conductivity and the Kapitza resistance at the interface of the electrical insulation with He II.

The heat transfer at the interface is seen as an energy exchange of phonons and their transmission through the He II-solid interface is governed by acoustics of continuous media. The thermal resistance results from the fact that not all the energy carried by the phonons can be transferred due to an acoustic mismatch between helium and solids. The heat flux, Q, going through the solid boundary is proportional to the difference in phonon energy density between the helium and solid material, which is proportional to $Q \propto T_s^4 - T_b^4$.

The Kapitza resistance at the surface of the sample in the inner bath, the resistance due to conduction, or the Kapitza resistance at the surface of the sample and the cryostat bath can all be used to define heat flux going through the sample Q_s. That is,

$$\frac{Q_s}{A} = \alpha(T_i^n - T_1^n) = \frac{\kappa}{\ell}(T_1 - T_2) = \alpha(T_2^n - T_b^n) , \tag{1}$$

where A is the total active area of heat transfer, ℓ, the thickness of the sample sheets, κ, the average thermal conductivity of sample, n, the exponent of the power law and α the Kapitza coefficient. T_b and T_i are respectively the temperature of the cryostat bath and the inner bath, and T_1 and T_2 are the unknown boundary temperatures at the interface given by the Kapitza boundary conditions. The order of the Kapitza power law n, given by the mismatch theory is 4 but experimentally, the value is found to vary between 3 and 5. In our data analysis we will keep n as a free parameter to compare our data with the theory. For temperature differences much smaller than the temperature of T_b or T_i, the Kapitza resistance on both side of the sample can be simplified to first order as:

$$\frac{Q_s}{A} = \alpha n T_i^{n-1}(T_i - T_1) = \frac{\kappa}{\ell}(T_1 - T_2) = \alpha n T_b^{n-1}(T_2 - T_b) . \tag{2}$$

Taking $R = A \cdot \Delta T / Q$ as the definition for thermal resistance, where ΔT stands for any temperature difference in a given medium, the thermal resistance of the sample, R_s, which is the sum of the two Kapitza resistances at the helium boundary and the resistance due to thermal conduction in the sheet, becomes

$$R_s = \frac{1}{\alpha n T_i^{n-1}} + \frac{\ell}{\kappa} + \frac{1}{\alpha n T_b^{n-1}} . \tag{3}$$

Note that R_s is a function of the inner and cryostat bath temperatures and the thickness of the Kapton sheet. Equation (3) can be simplified by linearization to give

$$R_s = \frac{2}{\alpha n T_b^{n-1}}\left(1 - \frac{1}{2}\frac{\Delta T}{T_b} + O(\Delta T)^2\right) + \frac{\ell}{\kappa} \approx \frac{2}{n\alpha}T_b^{1-n} + \frac{\ell}{\kappa} . \tag{4}$$

where ΔT is the total temperature difference across the sheets, $\Delta T = T_i - T_b$. Note that the second term on left end side of Equation (4) corresponds to 0.5% to 0.7% of the total resistance value in our experiment and will be neglected hereafter for simplicity. The first term on the right end side of Equation (4) is the Kapitza resistance whereas the second term is due to conduction.

To determine simultaneously the thermal conductivity and the Kapitza resistance, measurements of the same type of samples with different thicknesses have to be performed.

3.2.2. Experimental apparatus

The experimental set-up is composed of two support flanges and two sample holder flanges all made of stainless steel (see Figure 7). The tested material sample sheet has about 80 mm diameter of active heat transfer area and it is glued with Scotch-Weld DP190 epoxy resin to one of the holder flange (see Figure 8). The second holder flange pressures the glued area to ensure leak tightness of the connection. One of the support flanges comprises an open space, where a 1 Ω resistor (heater) and Allen Bradley (AB) type temperature sensor are located. The inner volume is fed with liquid helium and the wiring to the set-up instrumentation is introduced by a 0.5 mm inner diameter and 0.4 m long capillary tube, which is wrapped around the outside surface of the support flange and insulated in a epoxy resin block. The second support flange is blind and closes the inner helium volume. All set-up flanges are screwed together and surfaces between flanges are sealed with Scotch-Weld DP190 epoxy.
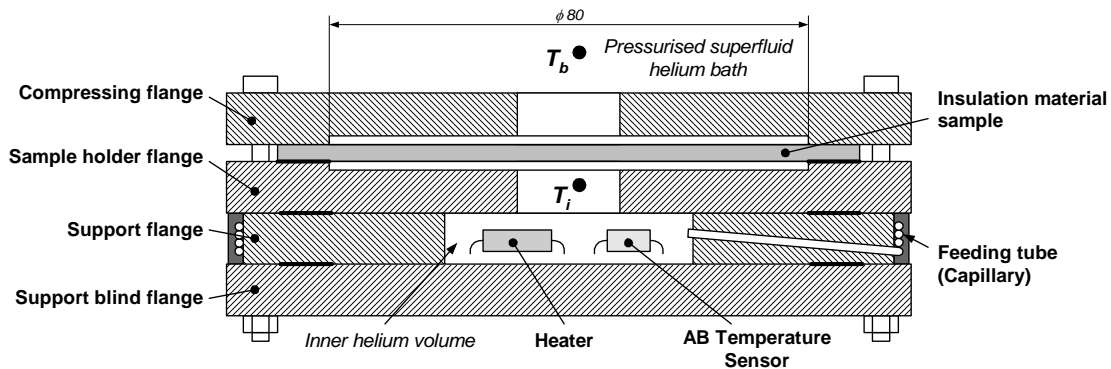

Figure 7. Schematic of the drum experimental set-up

3.2.3. Error discussion

The temperature of the pressurized cryostat bath, T_b, is monitored with a Cernox temperature sensor and maintained at the desired level by a LakeShore 332 Temperature Regulator. The calibration fit for He II temperature range gives at most a 0.2 mK difference between measurement and reference. In operation, the temperature of the cryostat bath is controlled to within 1 mK.

The Allen Bradley temperature sensor in the inner helium volume was calibrated in situ and a temperature – electrical resistance characteristic curve of the sensor was created before the experiment. The total accuracy of the AB sensor reading, included sensor calibration, the fitting curve errors and reading reproducibility, is round ±0.3 mK.

Heat dissipated in the inner volume is controlled by a Keithley 2400 Source Meter with an accuracy of 0.5% of the value. The total heat dissipated by the heater inside the inner volume is transferred to the saturated helium bath through the tested sample Q_s and by heat losses Q_{los}, which includes the capillary tube and the experimental setup walls heat transfer. The stainless steel heat losses were previously determined by a finite elements analysis method and do not exceed 2% of total heat flux. Calculation shows that for small temperature differences between inner volume and cryostat bath the capillary heat transfer is very high and reach up to 20% for $\Delta T < 1$mK. Nevertheless, the influence of the capillary heat loss is decreasing with increasing inner volume temperature. For ΔT higher than 10mK it is up to 2.5% of total heat flux [8].

The active area of heat transfer through the sample is delimited by the glue as it is shown in Figure 8. Therefore a photograph of the sample was taken and the real sample active area was computer-aid determined by a pixel counting method
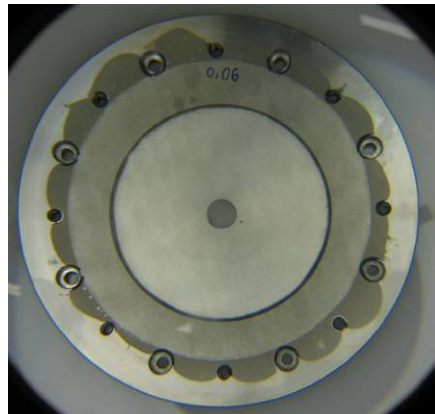
- 9 -

Figure 8. Photograph of the 55.5 μm thick sample. One can see the epoxy glue sealing the sample to the sample flange.

4. Experimental results

4.1.   Technical solution tests

This series of tests is aimed to acquire general understating and to validate some technical solutions that have been made for the design of the LHC magnets. We used the Saclay stack experiment to compare these different magnet configurations. The electrical insulation tested is all polyimide (Kapton) with a 1st layer of Kapton 200 HN (50 μm×11 mm) in 2 wrappings (no overlap) and a 2nd layer of Kapton 270 LCI (71 μm×11 mm) with a 2 mm gap. The polymerization had been performed at 60 MPa. This insulation was one of the candidates for the LCH magnet electrical insulation tested in the 90' [2]. The tests were performed with one heated conductor, the central one.

In the real magnet configuration, there is only one side of the coil, which is in direct contact with the pressurized helium at 1.9 K, which is located around the beam tube as depicted in Figure 9. The other side of the coil is in contact with the collars of the magnet. Therefore, it is obvious to think that there is one privileged heat path to cool the magnet through the side that is in contact with the helium layer around the beam tube connected to the heat exchanger.

The general idea behind these tests is to investigate the influence of the coil surface that is in contact with the pressurized helium and to compare the experimental results regarding the technical solutions that had been used at CERN.

We have performed three experiments with the Saclay stack with different configurations for one of the small faces of the stack as presented in the figure 10. The first experiment, which constitutes our reference, is the experiment with both small faces opened to helium. This configuration corresponds to the results in blue squares, which show the effect of helium in the insulation since the evolution of the temperature difference between the central conductor and the helium bath (ΔT) is not linear. With a "dry" insulation, i.e. without any helium, the curve would have been linear representing a conductive behaviour. The transition between superfluid helium and normal helium is also well seen in the figure 10 at a ΔT value of roughly 260 mK. This indicates that the helium in the conductor, close the thermometer, measures this singular phase transition of helium. This Q-ΔT curve shows a low overall thermal resistance where at 60 mW (corresponding to the LHC heat deposition due to beam losses) the ΔT is around 50 mK below the temperature margin for the LHC magnets.

The second test was performed with one face thermally insulated (red squares). The overall thermal resistance is higher since the heat has to travel through the entire stack to the cold

source. The results show roughly that the thermal resistance is two times higher than in the first configuration. This is somehow expected and the technical solution chosen in the design by CERN is to use an inner layer spacer made of G10 with some porosity as shown in Figure 11. The insulating piece creates channels for the helium and it improves the overall thermal resistance compare to the case where the one small face is thermally insulated. This is shown in the figure 10 with the green circle curve where this Q-ΔT curve is located between the two previous cases
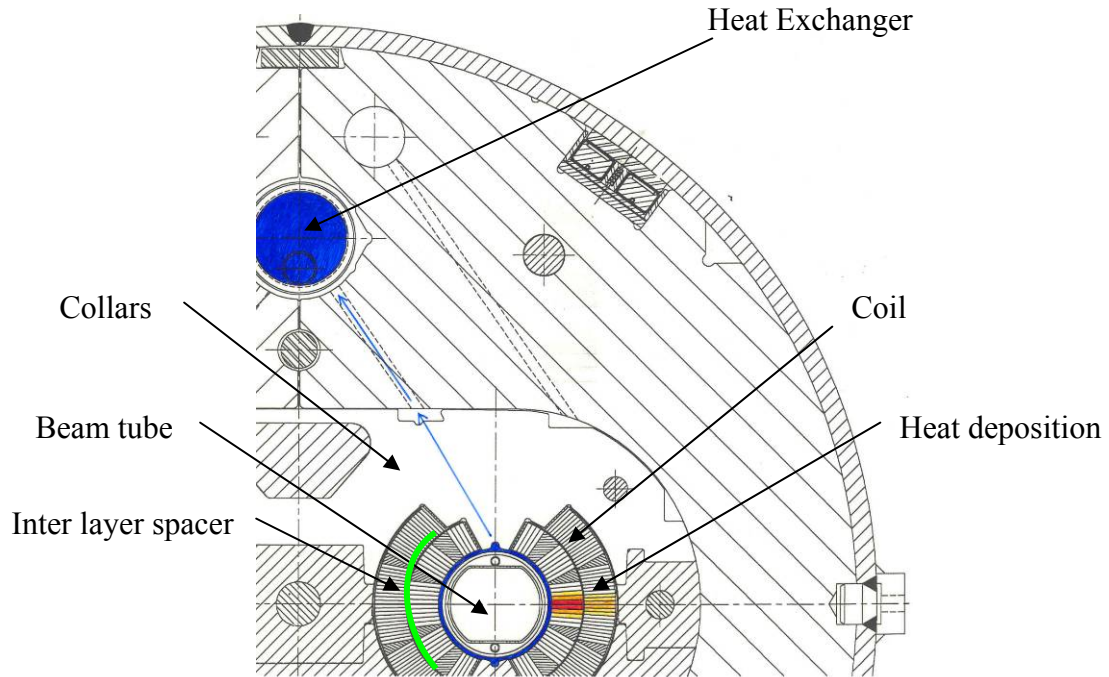
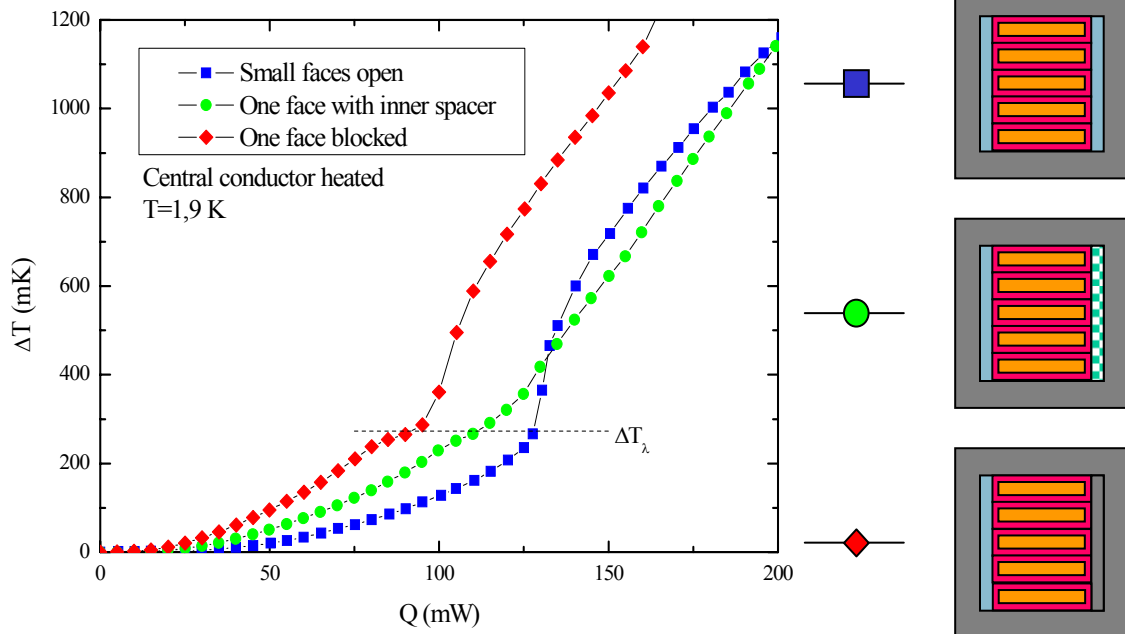Figure 9. Schematic of the LHC magnet cooling configuration

Figure 10. Experimental results with different small face configurations

The general understanding of the differences between the heat transfer curves can be explained by the fact that when one face is thermally insulated the heat path is longer, i.e. the heat dissipated in the half (insulated) side of the conductor has to travel through the cable and the insulation of large face to reach the helium. That is the proof that the quantity of helium and the "porosity" of the cable (conductor + insulation) is an important parameter in the heat transfer process for the cooling of the cable in an accelerator magnet. Finally we can conclude that the more helium paths exist, the larger quantity of helium in the cable is, the larger the heat transfer is and the better the cooling is. Obviously, in the construction of accelerator magnets this is a parameter that is hard to control and moreover increasing helium content in the cable probably goes against the magnetic design of such magnets.
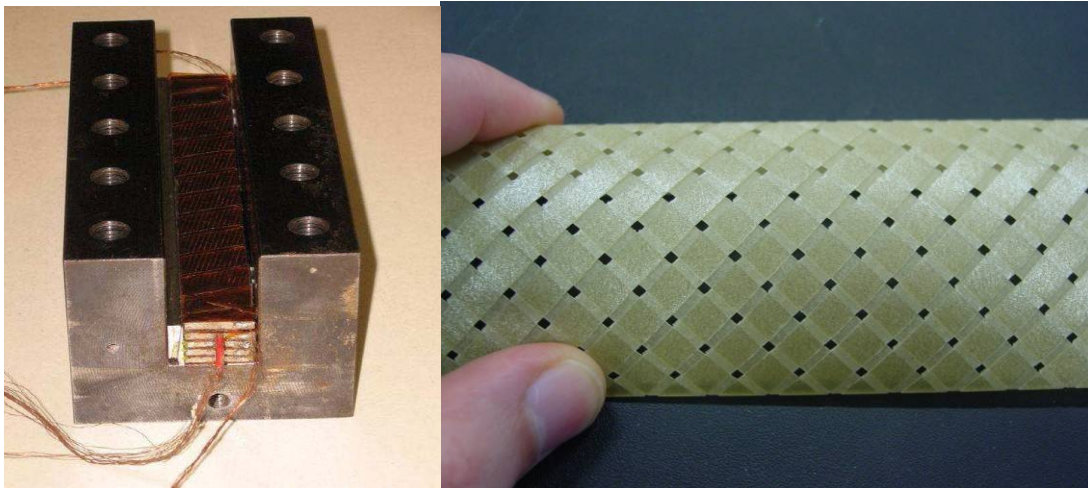

Figure 11. Stack experiment with sample. On the left picture, the sample with the thermally insulated face and on the right picture the inter layer spacer.

4.2.   Tests of the Conventional insulation

The conventional insulation made of fibreglass tape and epoxy resin developed by RAL [9] has been only tested in the drum experiment since this type of insulation is impermeable to helium [10]. Indeed a test in the coil configuration with the stack experiment would have given a thermal result driven by the thermal conductivity and the Kapitza resistance of the electrical insulation.

Figure 12 shows the results for different foils of the same material but with different thickness. For this test, four different thicknesses have been tested at different temperatures.

Figure 13 presents the total thermal resistance for the four different thicknesses at different temperatures of the bath. Each point of this graph is obtained from a ΔT-Q curve such as the one presented in Figure 14 for the 55.5 μm thick sample. At each temperature the slope of the curve ΔT-Q is determined from the measurement and constitutes the thermal resistance as,

$$R_s = \frac{A(T_i - T_b)}{Q_s} = \frac{A \cdot \Delta T}{Q_s} \tag{5}$$
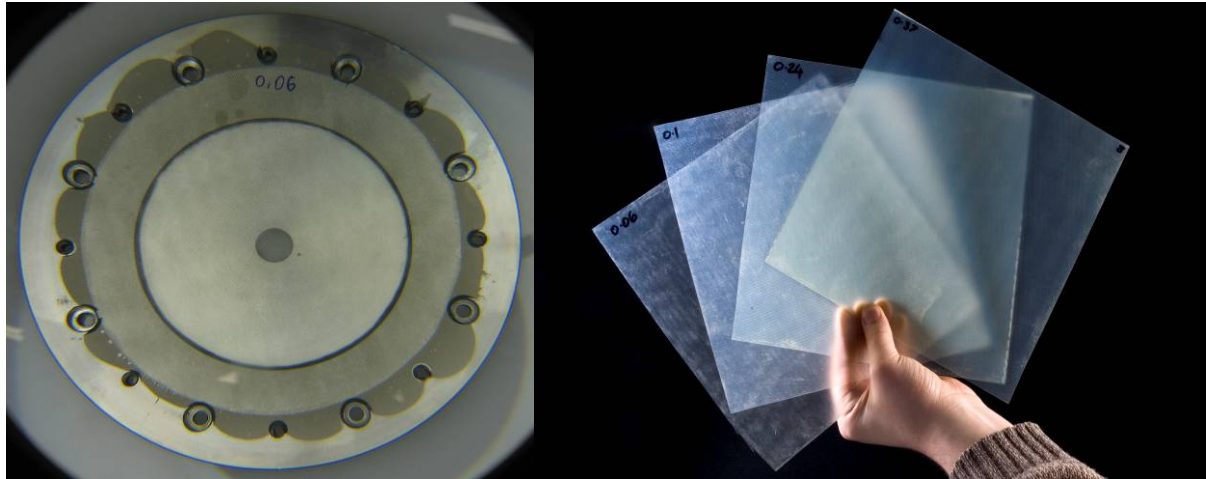
Figure 12. Pictures of the different samples tested.
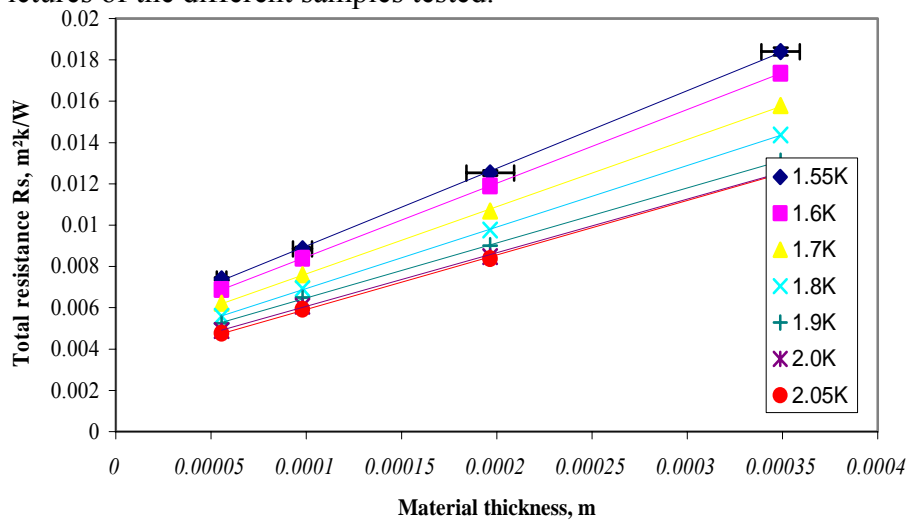

Figure 13. Total thermal resistance as a function of the thickness fir different bath temperature
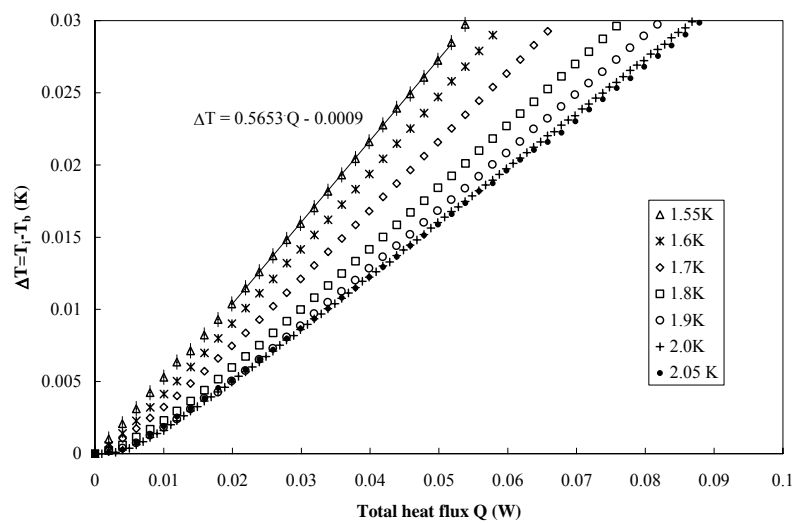

Figure 14. Evolution of the temperature difference across the sample with heat flux as a function of the bath temperature for the 55.5 μm thick sample.

The total thermal resistances are plotted as a function of the thickness and for each temperature the results are fitted by equation (4) from which the thermal conductivity and the Kapitza resistance can be extracted. Figure 15 presents the thermal conductivity of the conventional insulation and other materials such as epoxy resin, Kapton, Quartz glass and G10 [8, 11]. The innovative insulation thermal conductivity value is very close to the G10 and epoxy resin thermal conductivity; moreover the temperature dependency is also similar. This gives us good confidence in these results.

The evolution of the thermal conductivity is given by the following law,

$$k(T) = 0.00251.T + 0.00118 \text{ W/mK} \tag{6}$$

The Kapitza resistance is also extracted from the results in Figure 13 and is presented in Figure 16. To the best of our knowledge, these are the first results on Kapitza resistance on such materials. In Figure 16 the results are compared to the Kapitza resistance of Kapton [8], which is also a polymer and the results are similar.

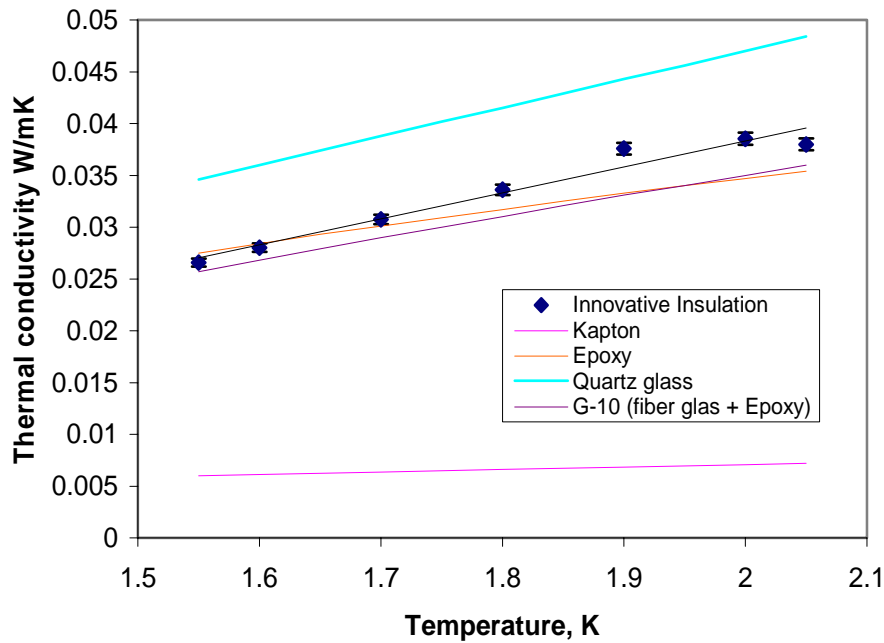$$Rk(T) = 0.0051.T^{-1.57} \text{ Km}^2/\text{W} \tag{7}$$

Figure 15. Evolution of the Thermal conductivity of the conventional insulation with temperature
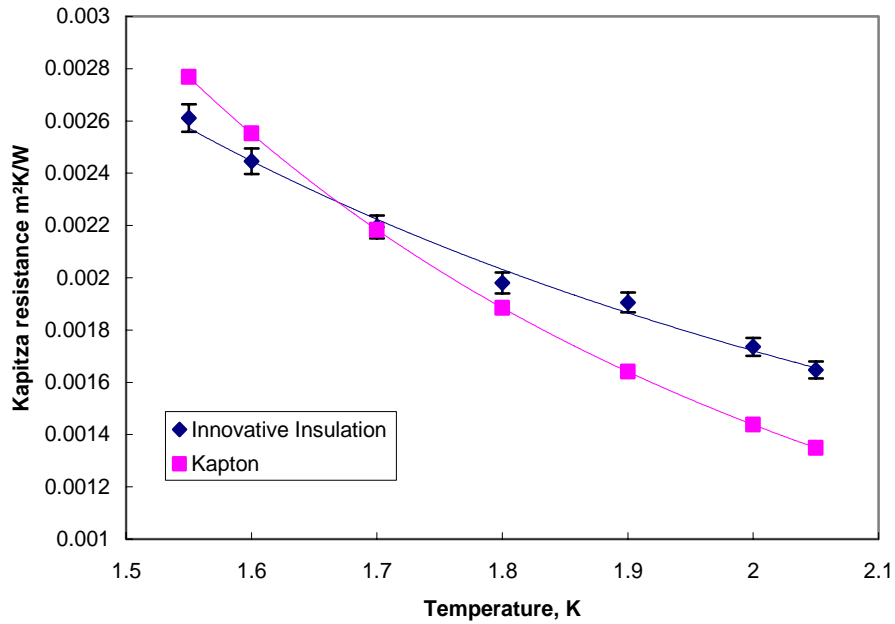
Figure 16. Kapitza resistance of the conventional insulation as a function of the temperature

4.3.   Tests of the innovative insulation

The innovative insulation developed at CEA Saclay [12] was tested with the stack experiment. The KEK stack set-up was used and after wrapping the insulation around the CuNi cables (cf. figure 17), a stack of five cables was heat treated for 50 hours at 666 °C at 10 MPa in order to activate the porous precursor and create the porosity in the innovative insulation. After the heat treatment, the thermometers were installed in the small holes by locally piercing the insulation. After the thermometer installation, the holes are filled up with epoxy resin to reduce the heat leaks from the thermometers location (cf Figure 17).
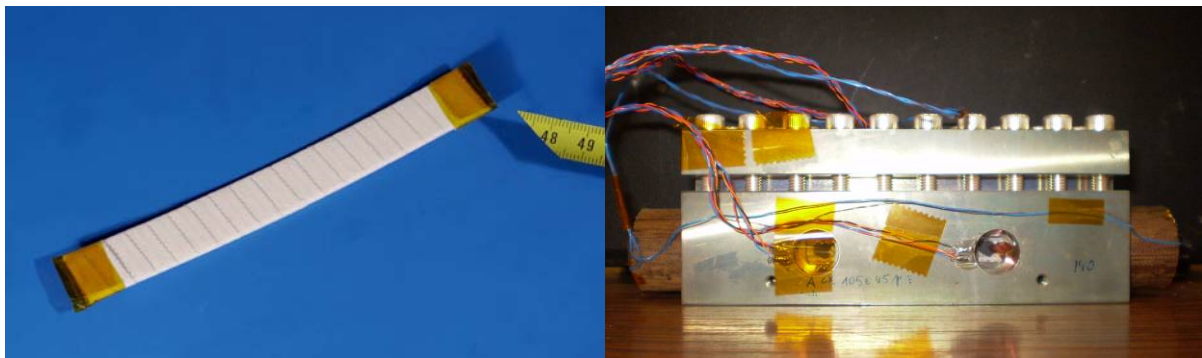

Figure 17. Dummy cable wrapped with the non reacted innovative insulation on the left picture and the fully instrumented stack experiment on the right picture.

All the CuNi conductors were heated as in the real magnet situation and the temperature of the central conductor was recorded.

Figure 18 represents the temperature difference between the central conductor and the bath temperature as a function of the heat dissipated in the cable. It is represented in W/m^3 and the volume represents the volume of the five conductors. Obviously the temperature increase is low and when compared to the results obtained during the R&D for the LHC magnet insulation [2], the ΔT is an order of magnitude lower. The beam losses in the current LHC

configuration correspond to 10 mW/cm^3 and the ΔT measured is around 5 mK whereas for the expected beam losses for the upgrade of LHC (between 50 mW/cm^3 to 80 mW/cm^3) the ΔT is around 20 mK.

These results constitute the first thermal test of a ceramic innovative insulation and show that this solution is suited to cool accelerator magnets subjected to beam losses as high as expected for the upgrade of the LHC. Nevertheless, measurements at higher mechanical loads close to the magnet constraint (100 MPa) are needed to confirm this positive result.
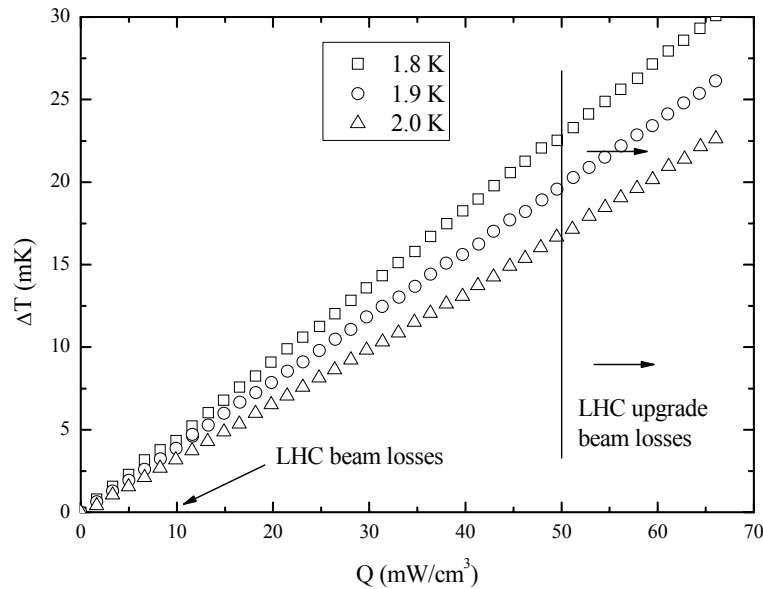

Figure 18. Central conductor temperature increase as a function of the heat dissipated in the five conductors for the innovative insulation

5. Acknowledgements

6. References

1. L. Burnod, D. Leroy, B. Szeless, B. Baudouy, and C. Meuris, Thermal modelling of the L.H.C. dipoles functioning in superfluid helium, **3**, Ed. (1994) 2295-2297

2. C. Meuris, B. Baudouy, D. Leroy, and B. Szeless, Heat transfer in electrical insulation of LHC cables cooled with superfluid helium, Cryogenics, (1999) 39 921-931

3. F. Michel, B. Baudouy, and H. Hervieu, "Technical Specifications for the pressurized He II cryostat (V.2) (task 2.2.1)," CEA Saclay 08/06/2004 2004

4. M. Chorowski, J. Polinski, B. Baudouy, F. Michel, and R. Van Weelderen, Optimization of the NED cryostat thermal shielding with entropy minimization method, Proceedings of the 21th International Cryogenic Engineering Conference, to be published, Ed. G. Gistau, (2006)

5. F. Michel and B. Baudouy, "Technical Specifications for the Sub-cooling Heat Exchanger," CEA Saclay 14/06/2004 2004

6. B. Baudouy, Etude des transferts de chaleur dans les isolations électriques de cables supraconducteurs d'aimant d'accélérateur refroidi par hélium superfluide, Thèse de doctorat de l'Université Paris VI, Université Paris VI, (1996)

7. N. Kimura, A. Yamamoto, T. Shintomi, A. Terashima, V. Kovachev, and M. Murakami, Heat transfer characteristics of Rutherford-type superconducting cables in pressurized He II, Ieee Transactions on Applied Superconductivity, (1999) 9 1097-1100

8. B. Baudouy, Kapitza resistance and thermal conductivity of Kapton in superfluid helium, Cryogenics, (2003) 43 667-672

9. S. Canfer, G. Ellwood, D.E. Baynham, F. Rondeaux, and B. Baudouy, Insulation Development for the Next European Dipole, IEEE Trans. on Magnetics, (2007) to be published

10. J. Polinski and B. Baudouy, Low temperature heat transfer properties of conventional electrical insulation for the Next European Dipole, presented and accepted for publication at the Cryogenics Engineering Conference 2007 in Chatanooga, AIP, Ed. J. G. Weisend, (2007)

11. E. Engineering, "Cryocomp," 3.06 ed. Florence SC, USA 29501: Cryodata Inc

12. A. Puigsegur, F. Rondeaux, E. Prouzet, and K. Samoogabalan, Development of an innovative insulation for Nb_3Sn wind and react coils, Advances in Cryogenic Engineering (Materials) **50A**, AIP, Ed. U. Balachandran, (2004) 266-272

7. Appendice 1 : CEC 2007 Publication

**LOW TEMPERATURE HEAT TRANSFER
PROPERTIES OF CONVENTIONAL ELECTRICAL
INSULATION FOR THE NEXT EUROPEAN DIPOLE**

J. Polinski[1], S. Canfer[2], G. Ellwood[2], B. Baudouy[1]

[1] CEA/Saclay, DSM/DAPNIA/SACM
     91191 Gif-sur-Yvette CEDEX, France

[2] Technology Department, STFC Rutherford Appleton Laboratory, Harwell
     Science and Innovation Campus, Didcot, Oxon, UK, OX11 0QX

ABSTRACT

The heat transfer properties of the fibreglass epoxy resin impregnated electrical insulation of the Next European dipole, known as conventional insulation, has been tested at low temperature. The electrical insulation is made of E-glass fibre with a plain weave and RAL epoxy system 227 (DGEBF epoxy resin and DETD aromatic hardener). The samples have been tested in pressurized superfluid helium (He II) where heat is applied perpendicularly to the fibres between 1.55 K to 2.05 K. Overall thermal resistance is determined with temperature and compared with other electrical insulation systems.

KEYWORDS: heat transfer, electrical insulation, helium 4 superfluid phase

INTRODUCTION

The Next European Dipole (NED) is a Joint Research Activity (JRA) of the Coordinated Accelerator Research in Europe (CARE) project, funded by EU-FP6 Research Infrastructures. CARE attempts the integration of high-energy-physics-related accelerator research and development (R&D) in Europe. The initial NED proposal had three main goals: to promote efforts among European laboratories involved in high-field accelerator magnet R&D, to promote the development of high-performance Nb_3Sn wires and cables in collaboration with European industry, to get ready for a luminosity upgrade of the Large Hadron Collider (LHC) [1].

One of the key issues in the operation of a superconducting particle accelerator is the temperature margin of the dipole and quadrupole magnets the most exposed to beam losses and the ability of the cryogenic system to cope with the deposited energies. In the case of the LHC, the temperature margins of the superconducting magnet coils operated in superfluid helium is mainly determined by the heat transfer coefficient through the Kapton insulation wrapped around the NbTi-based, Rutherford-type cables. Wherever NED-like magnets are implemented, they will be subjected to beam losses, and thereby, to energy depositions, which are likely to be higher than those presently foreseen in the LHC. Furthermore, 'wind and

react' Nb₃Sn coils call for the use of insulation materials and schemes that are very different from those applied in LHC magnets. Hence, the issues of heat transfer thought new electrical insulation systems must be investigated and overall thermal resistance of the material in superfluid helium conditions must be determined.

NEW CONVENTIONAL NED ELECTRICAL INSULATION

Glass-fibre epoxy sheets were produced using vacuum impregnation. This method mimics the vacuum impregnation of a magnet structure. However it should be noted that this produces an ideal material in that sheets were cured between flat mould platens, producing a consistent glass-epoxy fraction, whereas in a real magnet the insulation would be between cables which are not flat.

Plain weave glass fibre sheets were stacked between sheets of perforated polyester release film. The stack was placed in an aluminium foil tray and evacuated for 24 hours to a pressure of less than 0.1 mbar. A mixture of DGEBF epoxy resin, typified by Dow DER354, and DETDA hardener, typified by Albemarle Ethacure 100, was degassed in a separate vacuum chamber and stirred to break bubbles as it degassed. When a pressure of 0.1mbar was reached, the mixture was let up to atmospheric pressure. The epoxy mixture was flooded around the glass fibre sheets. When the level of epoxy resin covered the sheets, the vacuum chamber was let up to atmosphere. The stack was placed in a heated hydraulic press and cured at a pressure of 1MPa, at a temperature of 90ºC. When the epoxy was gelled the temperature was raised to 130ºC for 16 hours.

DESCRIPTION OF EXPERIMENT

Experimental method

The experimental method of determining the overall thermal resistance consists in measuring directly the temperature across samples as a function of heat flux [2,3]. In this method the sample sheet separates two different temperature helium volumes. The first helium volume is the superfluid pressurised bath of the cryostat, whereas the second volume is created inside of an experimental set-up. This volume is heated and its temperature T_i is higher than in the cryostat bath temperature T_b. In steady state condition the two volumes are isothermal with the high thermal conductivity of He II. With a known heat dissipation through the sample Q_s, cross sectional area of the sample sheet A and temperature difference ΔT between both volumes, a thermal resistance of the sample R_s can be determined by using following equation:

$$R_s = \frac{A(T_i - T_b)}{Q_s} = \frac{A \cdot \Delta T}{Q_s} \qquad (1)$$

Experimental apparatus

The experimental set-up is composed of two support flanges and two sample holder flanges all made of stainless steel (see FIGURE 1). The tested material sample sheet has a thickness of 0.073 mm and a diameter of 80 mm of active heat transfer area and it is glued with Scotch-Weld DP190 epoxy resin to one of the holder flange (see FIGURE 2). The second holder flange pressures the glued area to ensure leak tightness of the connection. One of the support flanges comprises an open space, where a 1 Ohm resistor (heater) and Allen Bradley (AB) type temperature sensor are located. The inner volume is fed with liquid helium and a wiring to the set-up instrumentation are introduced by a 0.5 mm inner diameter and 0.4 m long capillary tube, which is wrapped around the outside surface of the support flange and insulated in a epoxy resin block. The second support flange is blind and closes the inner helium volume. All set-up flanges are screwed together and surfaces between flanges are sealed with Scotch-Weld DP190 epoxy.
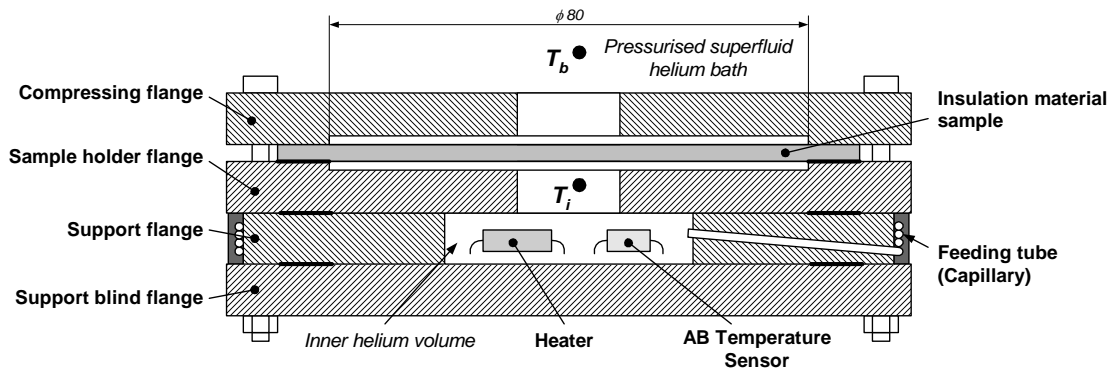

FIGURE 1. Schematic of the experimental set-up

Error discussion

The temperature of the pressurised cryostat bath, T_b, is monitored with CERNOX temperature sensor and maintained at desired level by LakeShore 332 Temperature Regulator. The calibration fit in the superfluid helium temperature range gives at most a 0.2 mK difference between measure and reference. In operation, the temperature of the cryostat bath is controlled with 1 mK.

The Allen Bradley temperature sensor in the inner helium volume was calibrated in situ and temperature – electrical resistance characteristic curve of the sensor was created before experiment. Total accuracy of the AB sensor reading, included sensor calibration, the fitting curve errors and reading reproducibility, is round ±0.3 mK.

Heat dissipated in the inner volume is controlled by KEITHLEY 2400 Source Meter with accuracy of 0.5% of the value. Total heat dissipated by the heater inside inner volume is transferred to saturated helium bath through tested sample Q_s and by heat losses Q_{los}, which includes the capillary tube and the experimental setup walls heat transfer. The stainless steel heat losses were previously determined by finite elements analysis method and do not exceed 2% of total heat flux [2, 3]. Calculation shows that for small temperature differences between inner volume and cryostat bath the capillary heat transfer is very high and reach up to 20% for $\Delta T < 1$mK. Nevertheless influence of the capillary heat loss is decreasing with increasing inner volume temperature. For ΔT higher than 10mK is up to 2.5% of total heat flux.
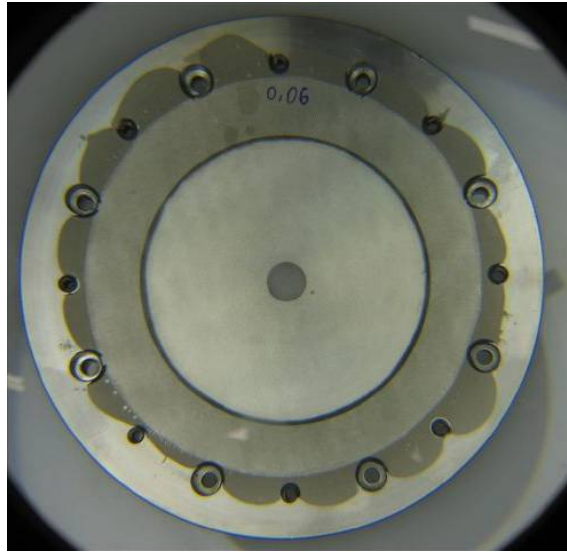
FIGURE 2. Photograph of the 0.073 mm thick sample. One can see the epoxy glue sealing the sample to the sample flange.

Active area of heat transfer through sample is delimited by the glue as it is shown in FIGURE 2. Therefore a photograph of the sample was taken and real sample active area was computer-aid determined by a pixel counting method as $0.004702 \pm 0.05\%$ m².

EXPERIMENTAL PROCEDURE, RESULTS AND COMPARISON WITH OTHER INSULATION MATERIALS

Measurements of the sample were performed in 7 different bath temperature from 1.55 K to 2.05 K. At a given temperature, applied heat was increasing by constant ramp value of 0.5 or 1 mW and the inner helium volume, T_i, and of the cryostat bath temperatures were measured at steady state condition. The time of stabilization of T_i was determined in pre-test as about 20 s, therefore time of each heat ramp was set as 30s.

FIGURE 3 shows results of the measurement as the temperature difference with heat flux at different temperature. At very low heat flux, one can see the effect of the capillary containing the instrumentation wires, where the ΔT-Q is not linear due to turbulent superfluid helium heat transfer. The effect of the capillary becomes negligible above few mW where the He II in it does not transfer heat sufficiently since the heat transfer cross sectional area is extremely small. The temperature dependence is clearly seen and the slope of the thermal characteristics decreases with temperature. This effect is due to the reduction of the Kapitza resistance with temperature (T^{-3} dependence) and the increase of the thermal conductivity of the epoxy resin and the fibreglass tape with temperature.

As mentioned in the previous section and as its can be clearly seen on FIGURE 3, for ΔT <10 mK influence of the capillary heat transfer on obtained result is very strong. However, for ΔT>30 mK Kapitza resistance value can be changed and provide additional uncertainties to future analysis. Therefore for determination of the material overall thermal resistance R_s, the results from ΔT =10-30 mK range are only taken in to account.
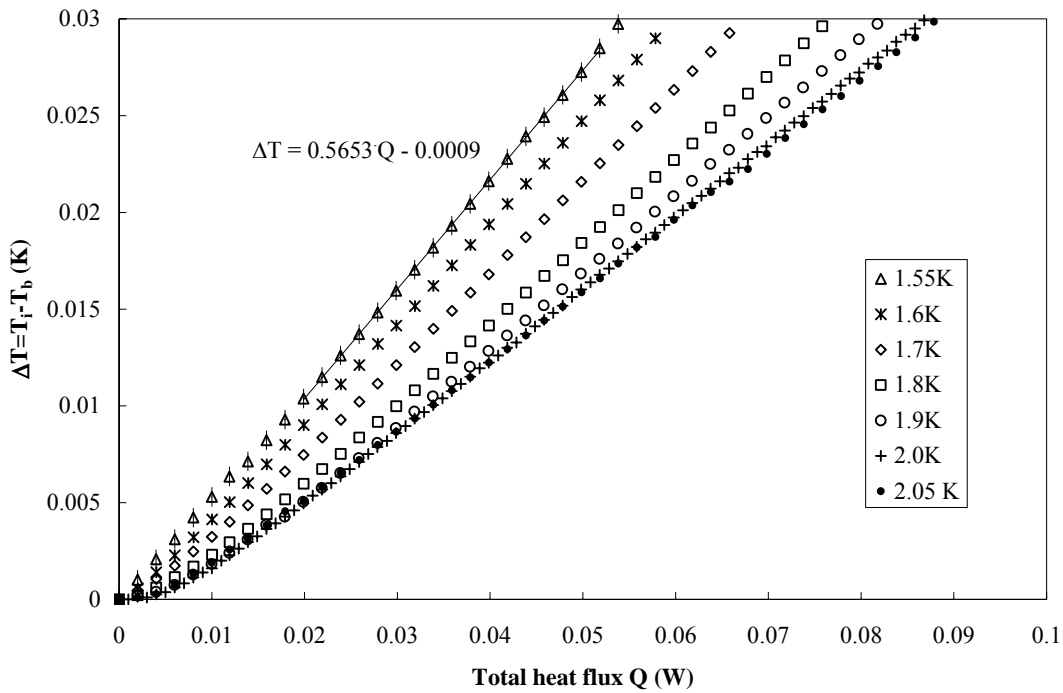
FIGURE 3. Evolution of the temperature difference across the sample with heat flux as a function of the bath temperature.
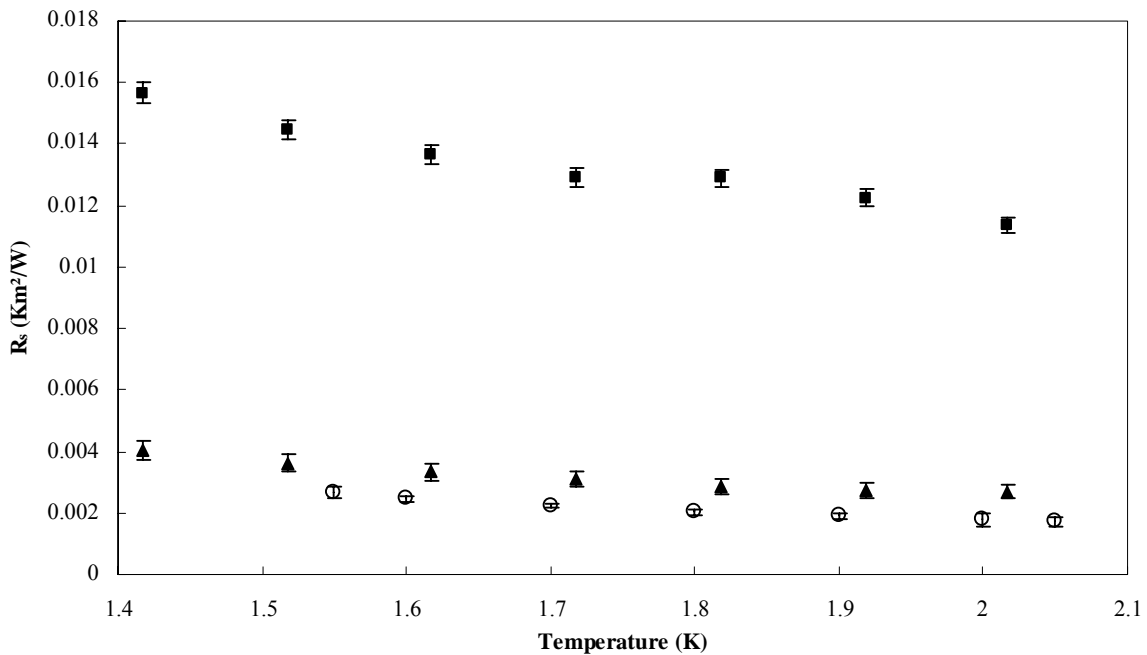

FIGURE 4. Overall thermal resistance of different electrical insulation materials. ○ - convectional insulation 0.073 mm, ■ – Kapton 0.077 mm [2], ▲ – Kapton 0.014 mm [2]

In consider $\varDelta T$ range each temperature characteristics can be approximated by linear function $a+bQ$ where b parameter is stand for the overall thermal resistance of the material R_s value divided by the active heat transfer area of the sample A. To find R_s value, fitting functions were constructed with the last square method for each bath temperature. An example of the fitting function and measuring errors is presented on FIGURE 3 for T_b=1.55 K case.

FIGURE 4 presents determined values of the overall thermal resistance of the NED convectional insulation for different bath temperature. As expected the total overall thermal resistance is decreasing with temperature. It is also shown on FIGURE 4 the value obtained for two different Kapton thicknesses [2]. One can see, that the R_s of the conventional NED insulation material is more then 5 times less than Kapton material with similar thickness and even better then Kapton with 5 times lower thickness. Assuming that the Kapitza resistance is identical to the Kapton, the explanation of this difference could come from the fact that the thermal conductivity of epoxy resin and G10 is about 5 times higher than the Kapton thermal conductivity. Anyway, to go into more details on the thermal performance of this insulation system at superfluid temperature, the thermal conductivity and the Kapitza resistance should be determined in measuring more samples with different thicknesses.

CONCLUSION

The thermal characteristics of 0.073 mm thickness of the E-glass fibre with a plain weave and RAL epoxy system 227 (DGEBF epoxy resin and DETD aromatic hardener) have been determined in superfluid helium. Comparison of the overall thermal resistance of this material with two different thicknesses of Kapton (which is presently used as NbTi superconducting cables electrical insulation) shows its very good thermal heat transfer properties. Therefore it can be considered as conventional electrical insulation of the NED Nb_3Sn superconducting magnet cables.

ACKNOWLEDGEMENT

REFERENCES

1. Devred, A. and al, *Supercond. Sci. Technol.* **19** pp. S67–S83 (2006)
2. Baudouy, B., *Cryogenics* **43** pp. 667–672 (2003)
3. Baudouy, B., Francois, M.X., Juster, F.-P. and Meuris, C., *Cryogenics* **40** pp. 127–136 (2000)